JOURNAL OF VIROLOGY, Mar. 2000, p. 2161–2168 Vol. 74, No. 5
0022-538X/00/$04.00+0

Sint1, a Common Integration Site in SL3-3-Induced T-Cell Lymphomas, Harbors a Putative Proto-Oncogene with Homology to the Septin Gene Family

ANNETTE BALLE SØRENSEN,[1] ANDERS H. LUND,[1]† STEEN ETHELBERG,[1]‡ NEAL G. COPELAND,[2] NANCY A. JENKINS,[2] AND FINN SKOU PEDERSEN[1,3]*

Department of Molecular and Structural Biology[1] and Department of Medical Microbiology and Immunology,[3] University of Aarhus, DK-8000 Aarhus C, Denmark, and Mammalian Genetics Laboratory, ABL-Basic Research Program, NCI-Frederick Cancer Research and Development Center, Frederick, Maryland 21702[2]

Received 26 August 1999/Accepted 7 December 1999

The murine retrovirus SL3-3 is a potent inducer of T-cell lymphomas when inoculated into susceptible newborn mice. Previously, DNAs from twenty SL3-3-induced tumors were screened by PCR for provirus integration sites. Two out of 20 tumors demonstrated clonal provirus insertion into a common region. This region has now been isolated and characterized. The region, named SL3-3 integration site 1 (*Sint1*), maps to the distal end of mouse chromosome 11, corresponding to human chromosome 17q25, and may be identical to a mouse mammary tumor virus integration site in a T-cell lymphoma, *Pad3*. Two overlapping genomic λ clones spanning about 35 kb were isolated and used as a starting point for a search for genes in the neighborhood of the virus integration sites. A genomic fragment was used as a hybridization probe to isolate a 3-kb cDNA clone, the expression of which was upregulated in one of two tumors harboring a provirus in *Sint1*. The cDNA clone is predicted to encode a protein which shows 97.0% identity to a human septin-like protein encoded by a gene which has been found as a fusion partner gene of MLL in an acute myeloid leukemia with a t(11;17)(q23;q25). Together these findings raise the possibility that a proto-oncogene belonging to the septin family, and located about 15 kb upstream of the provirus integration sites, is involved in murine leukemia virus-induced T-cell lymphomagenesis.

The induction of lymphomas and leukemias by the non-oncogene-bearing murine leukemia viruses (MLVs) is a complex process, comprising many steps of which the most well-defined one involves long terminal repeat (LTR) deregulation or impairment of cellular proto-oncogenes or tumor suppressor genes (29, 38). Proviral tagging of critical loci has during the last 15 years proved to be a powerful tool to identify genes associated with specific diseases. For example, c-*myb*, *Evi1*, and *Evi2* are genes/common integration sites which mainly are correlated with MLV-induced myeloid leukemias (4, 23, 33, 39), while c-*myc*, *Pim1*, *Mlvi1*/*pvt1*, *Evi3*, and *Evi5* primarily are associated with MLV-induced lymphomas (8, 13, 18, 21, 31, 37). Although there is no doubt that insertional mutagenesis plays a major role in tumor development, insertion into a common integration site for a specific tumor type has never been reported to be 100%, revealing the complexity of the process. Some proto-oncogenes (or common integration sites) may function redundantly as well as cooperate with other proto-oncogenes (17).

In addition to depending on the type of disease induced, the specific genes that will be tagged by a provirus depend on virus type. This is illustrated by the difference between SL3-3 MLV and Moloney MLV (Mo-MLV). Despite the fact that both viruses induce T-cell lymphomas with similar latency periods, the frequencies of integrations into specific sites are different. For example, while Mo-MLV and SL3-3 both exhibit insertions in the c-*myc* gene in 20 to 40% of the induced end-stage tumors, the frequencies of insertions observed in the *Pim1* locus amount to 15 to 65% of the Mo-MLV-induced tumors but less than 1% of the SL3-3-induced tumors (1, 8, 9, 15, 24, 29, 31, 35, 36). It thus appears that even viruses of similar disease specificities may exploit different gene activation pathways.

Previously, we have by a PCR-based method isolated and determined the sequences of provirus integration sites in twenty tumors induced by SL3-3 MLV (34, 35). We found that in two independent tumors a provirus had inserted into the same region. In essence, retroviral integration is random; thus the finding of two independent insertions into a common site strongly indicates that a linked host gene plays a role in the tumorigenic process.

We report here on further analysis of the integration site region as well as on the isolation of a cDNA clone representing a gene in this region. The chromosomal mapping of the region, which was named SL3-3 integration site 1 (*Sint1*), to the distal end of mouse chromosome 11 suggests that *Sint1* overlaps or is identical to the *Pad3* locus previously identified as an integration site in an mouse mammary tumor virus (MMTV)-induced T-cell lymphoma (28). Taken together with the finding that the associated *Sint1* cDNA seems to encode a protein homologous to a human septin-like protein that has been found as a fusion partner of MLL in an acute myeloid leukemia, this indicates that *Sint1* cDNA may identify a novel proto-oncogene involved in mouse T-cell lymphomagenesis.

* Corresponding author. Mailing address: Department of Molecular and Structural Biology, University of Aarhus, C. F. Møllers Allé, Bldg. 130, DK-8000 Aarhus C, Denmark. Phone: 45 8942 3188. Fax: 45 86 196500. E-mail: fsp@mbio.aau.dk.

† Present address: Division of Molecular Carcinogenesis, The Netherlands Cancer Institute, 1066CX Amsterdam, The Netherlands.

‡ Present address: Imperial Cancer Research Fund, Clare Hall Laboratories, South Mimms, Hertfordshire EN6 3LD, United Kingdom.

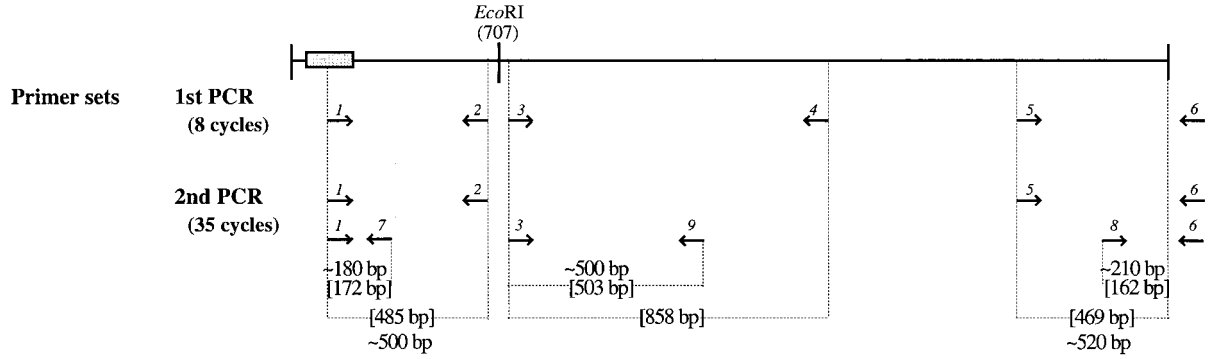

FIG. 1. Primer positions for RT-PCR analyses. The 3.0-kb *Sint1* cDNA is indicated as a line with the identified exon included as a shaded box. Arrows indicate positions and numbers of primers. The expected (brackets) and observed sizes of the PCR fragments are indicated. The PCR analyses were performed in two rounds (see Materials and Methods), and the products from the second PCR were analyzed by gel electrophoresis (not shown).

MATERIALS AND METHODS

Genomic DNA and RNA analyses. DNA was extracted from frozen tumor tissues as previously described (14). Tumors originated from experiments described by Hallberg et al. (14). Total RNA was isolated from frozen tumor tissues or cell lines by RNA Isolator (Genosys Biotechnologies, Inc.) following the manufacturer's recommendations.

For Northern analysis 25 μg of total RNA was separated on a 1.2% agarose–formaldehyde gel, transferred to nylon membranes (Zeta-Probe; Bio-Rad) by alkaline (50 mM NaOH) blotting, and hybridized in 0.5 M Na_2HPO_4 (pH 7.2)–7% sodium dodecyl sulfate buffer with ^{32}P-labeled (randomly primed DNA labeling) DNA probes. The multiple-tissue Northern and the mouse embryo Northern filters that were purchased from Clontech Laboratories, Inc., contain approximately 2 μg of poly(A)$^+$ RNA per lane. Hybridization procedures were as recommended by the manufacturer. The following probes were used: probe A, a genomic preintegration PCR probe (35); probe B, a genomic 900-bp *Pst*I fragment; probe C, a 700-bp *Eco*RI cDNA fragment; human β-actin, an internal control probe.

RNase protection assay. The assays were performed with the RPA III (RNase protection assay) kit from Ambion Inc. In essence, the supplied instruction manual was followed; 5 μg of tumor RNA and 10^5 cpm of RNA probe were used. The gel-purified radiolabeled RNA probes were made by in vitro transcription from T7 promoters according to standard protocols. The *Sint1* probe and the control mouse β-actin probe were transcribed from gel purified-PCR products using the following primers: *Sint1* probes 5′-GCA GTA AGC TTC CCC GAA TTC AAG GGA TCC ATT TAG GTG ACA CTA TAG AAC *CCT GGC TGA CAA CCC TAG AGA TGC CAT*-3′ (SP6) and 5′-TAC AGA AGC TTT ACA GAA TTC CAG GGA TCC TAA TAC GAC TCA CTA TAG GCG TA*A CTG TCA GCT TCA TTC GAA CCC CCT*-3′ (T7); mouse β-actin probes 5′-GCA GTA AGC TTC CCC GAA TTC AAG GGA TCC ATT TAG GTG ACA CTA TAG AAC CC*G CCC TAG GCA CCA GGG TGT GAT GGT*-3′ (SP6) and 5′-TAC AGA AGC TTT ACA GAA TTC CAG GGA TCC TAA TAC GAC TCA CTA TAG GCG TA*T CGG TGA GCA GCA CAG GGT GCT CCT*-3′ (T7). The underlined parts of the primers correspond to SP6 or T7 promoters, with the boldface letter denoting the transcriptional start site, while the italicized parts correspond to the hybridizing sequences of the primers. The expected sizes of the unprotected and RNase-protected RNA probes are as follows: *Sint1* probes, 378 and 325 bp, respectively; mouse β-actin probes, 263 and 210 bp, respectively. RNase-resistant products were analyzed by electrophoresis and autoradiography, and quantification of radioactive fragments was performed on the PhosphorImager SF (Molecular Dynamics, Inc.). Primers were from DNA Technology A/S, Aarhus, Denmark.

RT-PCRs. Reverse transcription-PCRs (RT-PCRs) were carried out using primer 10 (see below) for the first-strand cDNA synthesis (first-strand cDNA synthesis kit; Amersham Pharmacia Biotech) on approximately 2 to 4 μg of total RNA from tumors or spleen. PCR amplifications of the cDNAs were performed in two rounds. In the initial PCRs of eight cycles (first PCR; Fig. 1), 5 μl out of 15 μl of first-strand cDNA synthesis mixture was used as the template and the following primer sets were employed: 1 plus 2, 3 plus 4, and 5 plus 6 (Fig. 1). In the nested PCR (second PCR; Fig. 1) of 35 cycles, 2 μl out of 50 μl of the first PCR mixture was used as the template and the appropriate primer sets (1 plus 2, 1 plus 7, 3 plus 9, 5 plus 6, and 8 plus 6) were employed. For analysis, 10 μl out of 50 μl from the second PCR mixture was electrophoresed on an ethidium bromide-stained 2% agarose gel. The sequences of the primers were as follows: primer 1, 5′-TTGCAGCCAGCAGAGCCCACTTAAACT-3′; primer 2, 5′-TTC CTCCTGCAGGTACTTCTCATAT-3′; primer 3, 5′-CAGCGGATCACTGCA GACCTGCTGT-3′; primer 4, 5′-GGGCAGGCAGCTGAGGGCGCTGT-3′; primer 5, 5′-GCTAGCTTTCTGCAGCCCAGAAGT-3′; primer 6 (nested primer 10), 5′-GGGTCTAGAGCTCGAGTCACT-3′; primer 7, 5′-CTGCGCA TCTGCTCCAGGATGGAGT-3′; primer 8, 5′-CTGTTCGTCTCACCAGGCC GGTCCACGT-3′; primer 9, 5′-TGGGAAGAGATGGATGGAGGCAGGT-3′; primer 10 (poly[T] primer), 5′-GGGTCTAGAGCTCGAGTCACTTTTTTTTT TTTTTTTV-3′ (V = A, G, or C). All primers were purchased from DNA Technology A/S).

Library screening. The genomic library was made of partially *Mbo*I-digested mouse genomic (ES SV129 Dg) DNA inserted into *Bam*HI-digested λGEM12 vectors. Hybridizations with the preintegration PCR probe A and subsequent purifications of positive clones were done by standard techniques (30). Two positive clones were obtained. The cDNA library was a mouse embryonic cDNA library in a λZAP/EcoRI vector (Stratagene). Screening with probe B and in vivo excision (according to a protocol from manufacturer) resulted in one positive clone.

Sequence analysis. Sequencing reactions were performed with a Thermo Sequenase II dye terminator cycle sequencing kit (Amersham Pharmacia Biotech), and reaction products were analyzed on an automated DNA sequencer (373A DNA sequencer; Applied Biosystems Inc.). Nucleotide sequences were compared with sequences in the GenBank, EMBL, and EST databases by using Wisconsin package EGCG [version 8.1.0(a)] FASTA and BESTFIT programs.

Interspecific mouse backcross mapping. Interspecific backcross progeny were generated by mating (C57BL/6J × *Mus spretus*) F_1 females and C57BL/6J males as described previously (6). A total of 205 N_2 mice were used to map the *Sint1* locus (see below for details). DNA isolation, restriction enzyme digestion, agarose gel electrophoresis, Southern blot transfer, and hybridization were performed essentially as described previously (16). All blots were prepared with Hybond-N$^+$ nylon membrane (Amersham). The probe, a 392-bp fragment of mouse genomic DNA (probe A; Fig. 2) was labeled with [α-^{32}P] dCTP using a randomly primed labeling kit (Stratagene); washing was done to a final stringency of 0.5× SSCP (0.06 M NaCl, 7.5 mM sodium citrate, 10 mM sodium phosphate)–0.1% sodium dodecyl sulfate at 65°C. A fragment of 4.7 kb was detected in *Sph*I-digested C57BL/6J DNA, and a fragment of 3.8 kb was detected in *Sph*I-digested *M. spretus* DNA. The presence or absence of the 3.8-kb *Sph*I *M. spretus*-specific fragment in backcross mice was monitored.

A description of the probes and restriction fragment length polymorphisms (RFLPs) for the loci linked to *Sint1*, including *Grin2c*, *Hfh4*, and *P4hb*, has been reported previously (12). Recombination distances were calculated using Map Manager, version 2.6.5. Gene order was determined by minimizing the number of recombination events required to explain the allele distribution patterns.

Nucleotide sequence accession numbers. The nucleotide sequences of the *Sint1* cDNA (Fig. 6) and the genomic subclone shown in Fig. 5 have been assigned EMBL data bank accession no. AJ250723 and AJ250724, respectively.

RESULTS

Two proviruses inserted into a common region. Previously, in order to identify proto-oncogenes involved in SL3-3 MLV-induced T-cell lymphomagenesis, we have amplified by PCR and analyzed provirus integration sites in tumor DNAs (34, 35). In brief, from one such integration site of which the flanking sequence showed no homology to any known sequences in available databases, a unique PCR probe of 392 bp was generated (probe A; Fig. 2A). This probe was hybridized to Southern blots containing *Hin*dIII-digested DNA from 20 SL3-3-induced lymphomas, and thus the clonality of the original integration was verified. Moreover, the hybridization revealed

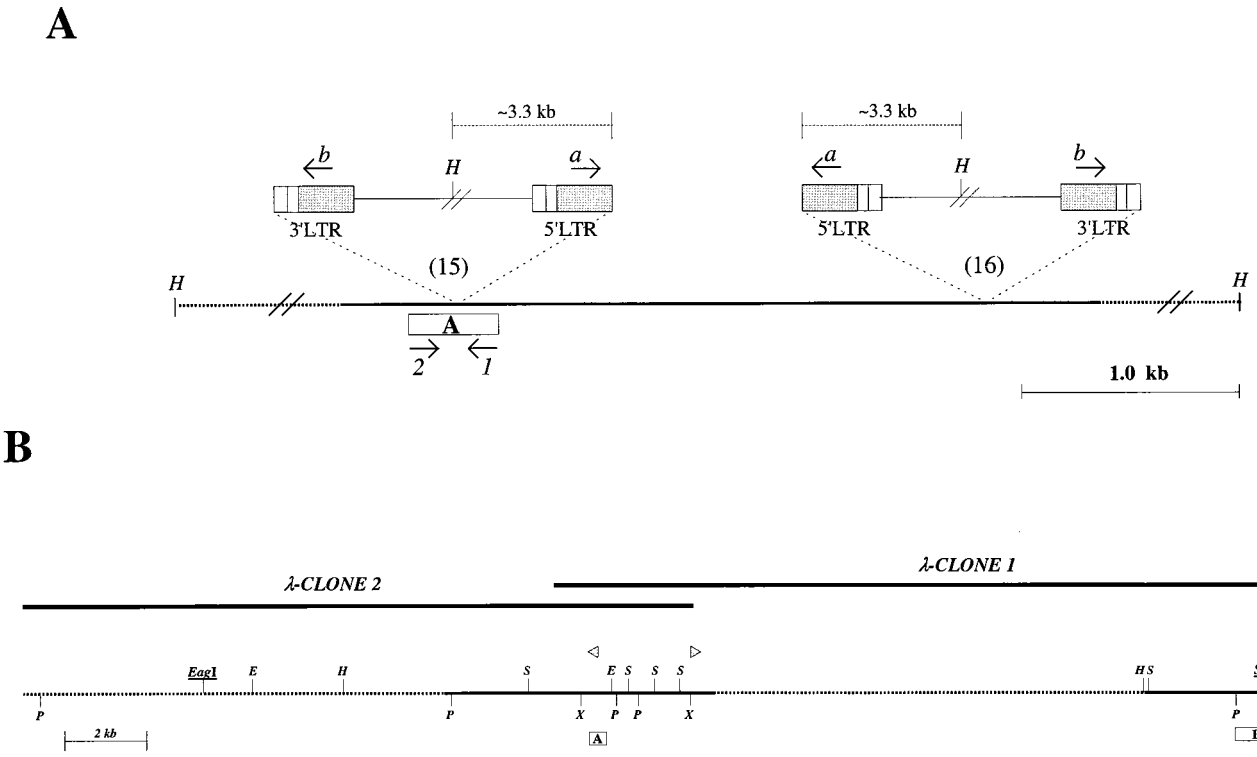

FIG. 2. (A) Relative locations and orientations of the integrated proviruses in two independent tumors (15 and 16). Box, preintegration site PCR probe A; arrows 1 and 2, primers used to amplify probe A; arrows a and b, provirus-specific primers; *H*, *Hin*dIII restriction site. (B) Restriction map of the cloned *Sint1* locus. Upper lines indicate the two overlapping genomic λ-phage clones, while the bottom line shows the resulting map. *Sac*I (S), *Xho*I (X), *Pst*I (P), *Hin*dIII (H), and *Eco*RI (E) sites are indicated. Underlined are the CpG indicator enzymes (see text). Dotted lines, regions only partly analyzed by restriction enzyme mapping and sequencing; boxes A and B, hybridization probes; triangles, provirus integration sites.

a rearranged fragment in the same region of DNA in an independent tumor (35). That this rearrangement was also due to an integrated provirus was confirmed by combinatorial PCRs using provirus-specific primers a and b together with primers 1 and 2 (primer localizations are indicated in Fig. 2A). A PCR fragment of about 3.0 kb was amplified by primer 2 and primer a. Taken together, these results demonstrated that a provirus had integrated into a common DNA region in two independent tumors, with the integration sites being separated by approximately 2.5 kb and the orientations of the integrated proviruses being opposite relative to each other (Fig. 2A). The DNA region was named SL3-3 integration site 1 (*Sint1*).

To obtain clones that covered the *Sint1* region, a genomic λ-phage library was screened with probe A. Two overlapping clones covering about 35 kb were obtained, and a physical map of *Sint1* was constructed (Fig. 2B).

Chromosomal mapping of *Sint1*. The integration site sequences did not reveal any open reading frames (ORFs), and the integration site probe (probe A; Fig. 2) did not hybridize to RNA from a murine T-cell line (data not shown), suggesting that the proviruses might have inserted outside an expressed region. Accordingly, the *Sint1* region could contain already-known proto-oncogenes. In order to test this, the chromosomal location of *Sint1* was determined by interspecific backcross analysis using progeny derived from matings of ([C57BL/6J × *M. spretus*]F_1 × C57BL/6J) mice. This interspecific backcross mapping panel has been typed for over 2,900 loci that are well distributed among all the autosomes as well as the X chromosome (6). C57BL/6J and *M. spretus* DNAs were digested with several enzymes and analyzed by Southern blot hybridization for informative RFLPs using probe A (Fig. 2). The 3.8-kb *Sph*I *M. spretus* RFLP (see Materials and Methods) was used to monitor the segregation of the *Sint1* locus in backcross mice. The mapping results indicated that *Sint1* is located in the distal region of mouse chromosome 11 linked to *Grin2c*, *Hfh4*, and *P4hh*. Although 108 mice were analyzed for every marker and are shown in the segregation analysis (Fig. 3), up to 147 mice were typed for some pairs of markers. Each locus was analyzed in pairwise combinations for recombination frequencies using the additional data. The ratios of the total number of mice exhibiting recombinant chromosomes to the total number of mice analyzed for each pair of loci and the most likely gene order are as follows: centromere–*Grin2c*–(2 of 147)–*Sint1*–(0 of 128)–*Hfh4*–(3 of 136)–*P4hb*. The recombination frequencies (expressed as genetic distances in centimorgans [cM] ± the standard error) were as follows: centromere–*Grin2c*–(1.4 ± 1.0, cM)–(*Sint1*, *Hfh4*)–(2.2 ± 1.3 cM)–*P4hb*. No recombinants were detected between *Sint1* and *Hfh4* in 128 animals typed in common, suggesting that the two loci are within 2.3 cM of each other (upper 95% confidence limit). This same region is known to include another retroviral integration site, *Pad3*, identified as an MMTV integration site in DNA from a T-cell tumor (28).

The distal region of mouse chromosome 11 shares a region of homology with human chromosome 17q25 (summarized in Fig. 3), suggesting that the human homolog of *Sint1* will map to 17q25 as well.

Identification of a *Sint1*-linked cDNA. To identify possible genes localized in the *Sint1* regions, the genomic λ clones were digested with the rare-cutting enzymes *Sac*II (CCGC↓GG), *Eag*I (C↓GGCCG), and *Bss*HII (G↓CGCGC). A cluster of sites for these enzymes would indicate the presence of CpG islands, which are associated with the promoter regions of

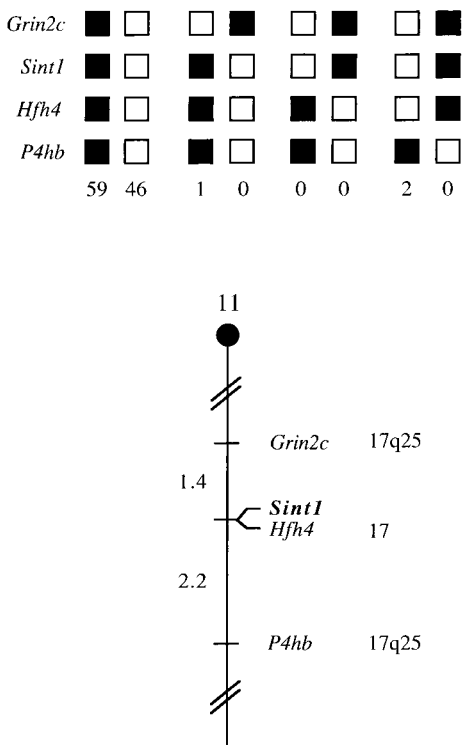

FIG. 3. *Sint1* maps in the distal region of mouse chromosome 11. *Sint1* was placed on mouse chromosome 11 by interspecific backcross analysis. The segregation patterns of *Sint1* and flanking genes in 108 backcross animals that were typed for all loci are shown at the top. For individual pairs of loci, more than 108 animals were typed (see text). Each column represents the chromosome identified in the backcross progeny that was inherited from the (C57BL/6J × *M. spretus*)F_1 parent. Black, boxes, presence of a C57BL/6J allele; white boxes, presence of an *M. spretus* allele. The number of offspring inheriting each type of chromosome is listed at the bottom of each column. A partial chromosome 11 linkage map showing the location of *Sint1* in relation to linked genes is shown at the bottom. Recombination distances between loci in centimorgans are shown to the left of the chromosome, and the positions of loci in human chromosomes, where known, are shown to the right. References for the human map positions of loci cited in this study can be obtained from the Genome Data Base, a computerized database of human linkage information maintained by the William H. Welch Medical Library of Johns Hopkins University (Baltimore, Md.).

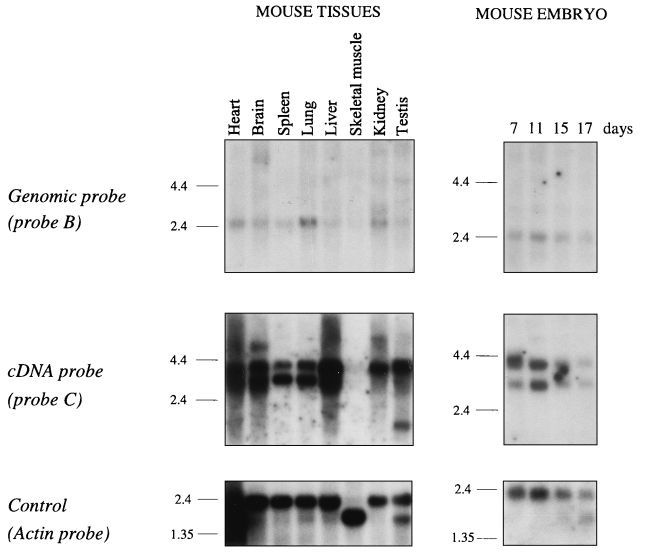

FIG. 4. Northern blot analyses of *Sint1* expression. All three panels are identical Northern blots hybridized with the probes indicated at the left. The blots contain about 2 μg of poly(A)$^+$ RNA per lane from eight different mouse tissues (left) and from mouse embryos at different time points (right). Size markers (in kilobases) are at the left of each autoradiogram.

many genes (2, 20). The restriction endonuclease digestions of the λ clones revealed no such cluster. However, both *Sac*II and *Eag*I cut once in the *Sint1* region as indicated in Fig. 2B. Since the *Sac*II cutting site is located very close to the end of genomic λ clone 1, it seemed possible that this site was part of a cluster of *Sac*II/*Eag*I/*Bss*HII cutting sites, and thus the 3.5-kb *Not*I/*Hin*dIII subclone of λ clone 1 became the starting point for a search for *Sint1* genes. From this subclone, a *Pst*I fragment (probe B; Fig. 2B) was isolated and used as a probe in Northern blot analyses with mRNA from different mouse tissues and from mouse embryos (Fig. 4). Although weakly expressed, a predominant transcript of about 2.4 kb was seen in all examined tissues except skeletal muscle. Probe B was then employed in an embryo cDNA library screen by which one cDNA clone of about 3.0 kb was obtained.

The sequences of the genomic 3.5-kb subclone as well as those of the cDNA clone were determined, and it was found that an exon of 132 bp with conserved 5′ and 3′ splicing signals is located in the genomic *Pst*I fragment (Fig. 5) and that the sites of the provirus integrations are located about 15 kb 5′ of this exon. The integrity and the 3′ end of the cDNA clone were verified by RT-PCRs employing primers located both inside and outside the identified exon as shown in Fig. 1, and the obtained PCR fragments all showed the expected sizes (data not shown).

To address the apparent discrepancy between the transcript size observed in the Northern blot analysis (~2.4 kb) and the size of the cDNA clone (~3.0 kb), a cDNA *Eco*RI fragment of a 700-bp (probe C; Fig. 5) was used as a probe on the same Northern blot (Fig. 4). This time two major transcripts of about 3.0 and 4.0 kb were seen in all examined tissues except skeletal muscle. However, in some tissues such as spleen and lung, the predominant transcript was the 3.0-kb species, whereas in other tissues such as kidney and testis, only the 4.0-kb transcript seemed to be expressed. The highest expression was seen in liver, where both mRNA species were found, although the 4.0-kb transcript was expressed at much higher levels. In addition, some minor transcripts were seen, e.g., a transcript of about 5.5 kb in brain and a transcript of about 1.4 kb in testis. Likewise, Northern blot analyses of RNA from different lymphoid cell lines with probe C showed different transcript sizes with the 3.0- and 4.0-kb transcripts as the predominant ones (data not shown). Thus, it appears that the overall RNA expression pattern of this gene is complex.

***Sint1* encodes a septin-like protein.** The sequence of the cDNA clone revealed a 5′-untranslated region (UTR) of at least 177 bp, an ORF of 1,002 bp, and a rather long 3′-UTR of 1,765 bp (Fig. 6). The 3′-UTR contains several copies of the ATTT(A) motif, which is thought to confer instability to mRNAs (10, 32), and a consensus poly(A) signal (AATAAA). The ORF is predicted to encode a polypeptide of 334 amino acid (aa) residues.

A comparison of the predicted amino acid sequence encoded by the *Sint1* cDNA clone and sequences in the GenBank, EMBL, Swissprot, and EST databases showed a significant identity (97.0%) to a human brain cDNA-encoded protein and the human MSF (MLL septin-like fusion) protein (27) (Fig. 7). The comparison analyses in addition revealed significant homologies (>70% identity) to proteins of the septin family, a family of proteins which were originally identified

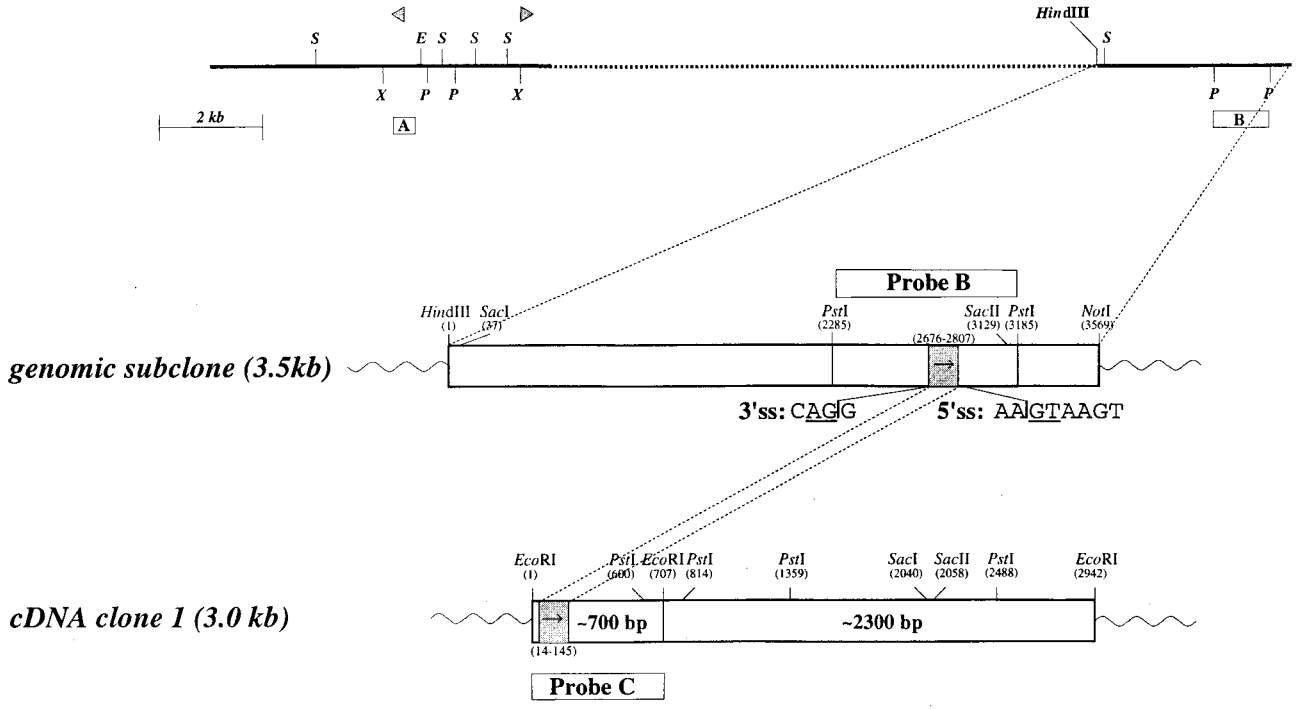

FIG. 5. Correlation between *Sint1* genomic region and *Sint1* cDNA. (Top) Part of the genomic region; (middle) genomic 3.5-kb *Hin*dIII/*Not*I subclone; (bottom) corresponding cDNA clone. Triangles, provirus integration sites. Restriction enzyme site abbreviations are as defined for Fig. 1. Hybridization probes are shown as boxes A, B, and C. The grey box containing an arrow indicates the location and orientation of the exon in the genomic clone as well as in the cDNA clone. The 5′ and 3′ splicing signal (ss) sequences are shown with the conserved intron dinucleotides underlined.

by analysis of budding yeast cell division cycle mutants defective in cytokinesis (5, 22) and which were later isolated from flies, mice, and humans (19, 25, 26). The amino acid sequences of these proteins contain motifs that define the GTPase superfamily (3), although the function of nucleotide hydrolysis has not been determined. As indicated in Fig. 7, the GTP-binding motifs are also conserved in the *Sint1* cDNA-encoded protein.

***Sint1* cDNA expression in tumors with proviral insertions at the *Sint1* locus.** In order to examine if provirus integrations at the *Sint1* locus affected the expression of the *Sint1* cDNA, an RNase protection assay was performed with RNAs from seven different SL3-3-induced tumors, including the two tumors (tumor no. 15 and 16) that harbor a clonal provirus insertion at the *Sint1* locus (Fig. 2). The RNA probe employed spans 325 bp of the coding region of the *Sint1* cDNA (Fig. 8). When the intensities of the protected *Sint1* fragments were correlated with the intensities of the protected internal control fragments (mouse β-actin), a clear upregulation (two- to threefold) of the *Sint1* cDNA expression in tumor 15 was observed (Fig. 8). This indicates that a provirus integration at the *Sint1* locus may have modified the expression of the linked *Sint1* gene, the effect of which might have contributed to the development of the tumor. On the other hand, no significant alteration of the expression level of the *Sint1* gene could be detected in tumor 16, which may suggest a more complex mode of involvement of the *Sint1* gene in tumor progression.

DISCUSSION

In order to identify genes involved in T-cell lymphomagenesis, we have analyzed provirus integration sites in SL3-3-induced T-cell tumors. We have identified a region of the mouse genome which has been rearranged by a retrovirus insertion in 2 of 20 tumors. Hence, this locus, which we have named *Sint1*, appears to define a region that is important in the development of T-cell lymphomas. This is further supported by the findings of Rajan and Dudley (28), who identified an integration site, named *Pad3*, in an MMTV-induced T-cell lymphoma. *Pad3* cosegregates with the marker *Hfh4* (HNF-3/forkhead homolog 4) as does *Sint1* (Fig. 3); hence *Sint1* and *Pad3* may constitute the same locus.

A genomic fragment was used as a probe to isolate a linked cDNA clone of 3 kb. Enhanced levels of expression of this cDNA were detected in one of the two tumors carrying a proviral insertion in the *Sint1* locus, strongly indicating that in this case overexpression of the *Sint1* gene, probably due to the integrated provirus, did play a role in tumor initiation and/or progression. Regarding the other tumor harboring a provirus in the *Sint1* locus, the picture is less clear, since no change of expression was detected. As the normal expression pattern of the *Sint1* gene during differentiation is not known, there are several possibilities concerning how and when the *Sint1* gene may be affected by the integrated provirus. For example, the distinction between regulated and deregulated expression levels may at certain stages be subtle, and a disturbance by an integrated provirus may have profound effects on differentiation and/or growth but may not necessarily have measurable effects on the expression level in the end-stage tumor.

The distance of approximately 15 kb between the integrated proviruses and the identified *Sint1* exon and the fact that the two proviruses have integrated in opposite directions relative to each other indicate that the mechanism of activation is of the type referred to as enhancer insertion (29, 38). In addition, preliminary Northern blot analyses show no detectable differences in transcript sizes in RNAs from tumors harboring proviruses inserted at the *Sint1* locus and from other tumors (data

```
   1  AATTCGGCACGAGGCGCCAGAACACAACCGGAGTCCCTGAGGCTCCAGAACAGAGTCAGG
  61  GTGAGCCAGCCCCAGCCCAGCCCCAGGTTCTGGCTTCCTCTCTTGCTTCTCCCTCCTTTG
 121  GTTGCAGCCAGCAGAGCCCACTTAAACTCCGAGGTGACTCCCAGCTGTGTTGGCGACATG
                                                              M
 181  GCTGACAACCCTAGAGATGCCATGCTCAAGCAGGCCCCCGCGTCACGGAACGAAAAGGCC
       A  D  N  P  R  D  A  M  L  K  Q  A  P  A  S  R  N  E  K  A

 241  CCCATGGAGTTCGGCTATGTGGGGATCGACTCCATCCTGGAGCAGATGCGCAGGAAGGCT
       P  M  E  F  G  Y  V  G  I  D  S  I  L  E  Q  M  R  R  K  A

 301  ATGAAACAGGGCTTCGAGTTTAACATCATGGTGGTTGGGCAGAGCGGCCTCGGGAAGTCC
       M  K  Q  G  F  E  F  N  I  M  V  V  G  Q  S  G  L  G  K  S

 361  ACTTTAATCAATACCCTCTTCAAGTCCAAAATCAGCCGGAAGTCGGTGCAGCCCACCTCG
       T  L  I  N  T  L  F  K  S  K  I  S  R  K  S  V  Q  P  T  S

 421  GAGGAACGCATCCCCAAGACGATCGAAATCAAGTCGATCACCCACGATATTGAAGAGAAG
       E  E  R  I  P  K  T  I  E  I  K  S  I  T  H  D  I  E  E  K

 481  GGGGTTCGAATGAAGCTGACAGTGATTGACACGCCGGGCTTCGGAGACCACATCAACAAT
       G  V  R  M  K  L  T  V  I  D  T  P  G  F  G  D  H  I  N  N

 541  GAGAACTGCTGGCAGCCCATTATGAAGTTCATCAATGACCAATATGAGAAGTACCTGCAG
       E  N  C  W  Q  P  I  M  K  F  I  N  D  Q  Y  E  K  Y  L  Q

 601  GAGGAAGTCAACATCAACCGGAAGAAGCGCATTCCCGACACCCGTGTCCACTGCTGCCTC
       E  E  V  N  I  N  R  K  K  R  I  P  D  T  R  V  H  C  C  L

 661  TACTTCATCCCAGCCACCGGCCACTCGCTCAGGCCCCTGGACATTGAATTCATGAAGCGC
       Y  F  I  P  A  T  G  H  S  L  R  P  L  D  I  E  F  M  K  R

 721  CTAAGCAAAGTGGTGAACATTGTCCCAGTCATCGCCAAGGCTGACACGCTGACCCTGGAG
       L  S  K  V  V  N  I  V  P  V  I  A  K  A  D  T  L  T  L  E

 781  GAGAGGGTCTACTTCAAACAGCGGATCACTGCAGACCTGCTGTCCAACGGCATTGACGTG
       E  R  V  Y  F  K  Q  R  I  T  A  D  L  L  S  N  G  I  D  V

 841  TACCCGCAGAAGGAGTTTGATGAGGACGCAGAAGACCGGCTGGTGAACGAAAAGTTCCGG
       Y  P  Q  K  E  F  D  E  D  A  E  D  R  L  V  N  E  K  F  R

 901  GAGATGATCCCATTTGCTGTGGTGGGCAGCGACCATGAGTATCAAGTCAATGGCAAGAGG
       E  M  I  P  F  A  V  V  G  S  D  H  E  Y  Q  V  N  G  K  R

 961  ATTCTGGGAAGGAAGACCAAGTGGGGCACTATCGAAGTTGAGAATACCACTCACTGTGAA
       I  L  G  R  K  T  K  W  G  T  I  E  V  E  N  T  T  H  C  E

1021  TTTGCTTACCTGCGGGATCTCCTTATCAGGACGCACATGCAAAACATCAAAGACATCACC
       F  A  Y  L  R  D  L  L  I  R  T  H  M  Q  N  I  K  D  I  T

1081  AGCAACATCCACTTCGAAGCCTACCGAGTGAAACGCCTCAACGAGGGCAACAGCGCCATG
       S  N  I  H  F  E  A  Y  R  V  K  R  L  N  E  G  N  S  A  M

1141  GCCAACGGGATCGAGAAGGAGCCGGAAGCCCAGGAGATGTAGATGCGTCCCGCCCCTGGA
       A  N  G  I  E  K  E  P  E  A  Q  E  M  *

1201  CCCCACCCCCAGATCTTTTCATCATCCCTGGCCCACCCACCTACCCTGTCTTATTTTATA
1261  TAATTATCTCCTTGTCACCTGCCTCCATCCATCTCTTCCCACACTTTGCCAGGTAACAAG
1321  AGAGGGTTTACCTCCCAAGTGTGCTCTTATTGGCTGCAGCAGCAGGGTGGGCGGGGCTAA
1381  GCCTGGGCTTGCCTCTGTGCTCTATTTCCACCCGGGCTCAGCCCCTGAGGGGTTAGAAGA
1441  GCTATGTGTCCGTCCCCCGCTCTGAGTTCTAAGCTGAAGCCTGTGGGGGCCAAGTCCTAG
1501  GGGGTGCAGAGGAGCCCGTTAGACCACAAGACCCCATGGCCGCAGCCTCAAGCAGGTTAG
1561  AGACTGCCCCAAAGGAGGATGGAGCTGGCCGGGTATTCCTGAAACCTCACCTGCCCCTCC
1621  GGGGGCGTTTCTTACAGCGCCCTCAGCTGCCTGCCCCTCAAGGGAACTAGAGGCGTCACA
1681  GCCAAAGTTGCCAATCACTTAGACAAAGTGACAACCGTGCCCCTCGAGCTTGTCCCAGAG
1741  CAGAAAGTGCCTTGATCTACAAGAGCCAGTCACCTCTTCCCAGATGTCCCTTTGGGTGAA
1801  AAGCAGGGACGTGCTGGAGAGAGGGAGGTATCTTTTCTCCCTCGCCCTTGGGTTCTCTCT
1861  CCCCTGTGCTGTAGATATCGCTACTACACTGGGCTTTAATTATAAAAGACGAAGCGTGAA
1921  AGATGCTCCCCGATGTTAGGAAGCCCCGCCCCCAATGTAAGGAAGGTCAAAGCAAGAAGA
1981  TGAGTCGAAGCCATGAGGGAGGAAGCCGTGGAAGGGAGGCATAAGAGTGTGTGGGAGCTC
2041  TCCTGCCCAGGTGCCGCGGAAGGCATATCCGCGTGGTCCTCAGTTTGGGCCAAGATATTC
2101  TGGTTACATTGATGCTCCGCTGCCTCACCCTGTCCCACCCCACACACCCCAGGCTCAAGC
2161  CTTGATGATTCAGTGACTGTACTGGGTGGGAGCCAGAAACCTGACCATTTTGTTGTCTAC
2221  ATGAGCCTAGACTAGCCCTGTGCCCCAGAACCCATCAAAAATACCCCTAAAGAGGGAAAG
2281  ATGAGGGGGTCAGAGATGGATAGCCAGGCTCACTCATCTTCTCTCAGAGGGAACATTAGG
2341  GACCATCCATGCACAGCTGACCAAAGCCGTGTCCTTCCTGCCTGCCTCCCATTCTCATTT
2401  GCCCCTGAGGAGAAAGTTTGGTGAGGTGCGTTAGGTTGGACCCGCTTGGGGAAGGTGCCT
2461  CTACAGACCCAGGGCTAGCTTTCTGCAGCCCAGAAGTGCAGTGGGAGGGGTGGGGTGCAG
2521  ACAGATGGAGACGAACATTGTTTCCTGCTTTGGGCGTCTACTCCCTCATCCAAGCATGGA
2581  AGGGCCCCTCGTCATGCCCTGTGGCCGAACAGTTCGCTTGCCAGCTTGCCAAGTTCTTTG
2641  CCAAAATCAGGACTTTGAAGGAAATCTCCAGCACGCTGGACCCAGGGCACTCCGGCCTTC
2701  ACCAGCCCAAGTGACCCTGGGGATTTAGCAGCAACCCGGTCATCAGGATGACTTTGTGCC
2761  TCTGTAACCAGGTATTGAAACTGTTCGTCTCACCAGGCCGGTCCACGTGGCCCTCTGCTG
2821  GGGGCTTCCTGGTGGGGGGGCAGAAAAGTCTCTCTCTCTCTCTCTCTCTTTTTTTTTT
2881  TGTATAAATAACAAAGTGTCTGAAATGTATTTCCTGAAATAAATGTTTCAAATCTCGTGC
2941  CG
```

FIG. 6. *Sint1* cDNA and predicted amino acid sequences. In the 3′-UTR, the AT degradation motifs are underlined and the polyadenylation site consensus sequence is boxed.

not shown). However, since the integrity of the *Sint1* cDNA 5′ end has not been verified, the possibility still exists that the proviruses have integrated in an intron of the *Sint1* gene and thereby, at least for tumor 16, which harbors a provirus inserted in the same transcriptional orientation as that of the *Sint1* gene, the activation could have been 3′-LTR or 5′-LTR promotion in which a 5′ exon(s) might have been removed from the resulting transcript.

The putative *Sint1* cDNA-encoded septin-like protein of 334 aa revealed a striking homology (97.0% identity; Fig. 7) to the encoded protein (568 aa) of MSF, a fusion partner gene of MLL in an acute myeloid leukemia with a t(11;17)(q23;q25)

```
Sint1            1 MADNPRDAMLKQAPASRNEKAPMEFGYVGIDSILEQMRRKAMKQGFEFNI 50
                   ||| |||| ||||||||||||.:|||||||||||||||||||||||||||||
KIAA0991/MSF    88/234 MADTPRDAGLKQAPASRNEKAPVDFGYVGIDSILEQMRRKAMKQGFEFNI 137/283
                       .    .    .    .    .    .    .    .    .    .

Sint1           51 MVVCQSGLGKSTLINTLFKSKISRKSVQPTSEERIPKTIEIKSITHDIEE 100
                   ||||||||||||||||||||||||||||||||||||||||||||||||||||
KIAA0991/MSF  138/284 MVVGQSGLGKSTLINTLFKSKISRKSVQPTSEERIPKTIEIKSITHDIEE 187/333
                       .    .    .    .    .    .    .    .    .    .

Sint1          101 KGVRMKLTVIDTPGFGDHINNENCWQPIMKFINDQYEKYLQEEVNINRKK 150
                   ||||||||||||||||||||||||||||||||||||||||||||||||||||
KIAA0991/MSF  188/334 KGVRMKLTVIDTPGFGDHINNENCWQPIMKFINDQYEKYLQEEVNINRKK 237/383
                       .    .    .    .    .    .    .    .    .    .

Sint1          151 RIPDTRVHCCLYFIPATGHSLRPLDIEFMKRLSKVVNIVPVIAKADTLTL 200
                   ||||||||||||||||||||||||||||||||||||||||||||||||||||
KIAA0991/MSF  238/384 RIPDTRVHCCLYFIPATGHSLRPLDIEFMKRLSKVVNIVPVIAKADTLTL 287/433
                       .    .    .    .    .    .    .    .    .    .

Sint1          201 EERVYFKQRITADLLSNGIDVYPQKEFDEDAEDRLVNEKFREMIPFAVVG 250
                   ||||:||||||||||||||||||||||||.|||||||||||||||||||||
KIAA0991/MSF  288/434 EERVHFKQRITADLLSNGIDVYPQKEFDEDSEDRLVNEKFREMIPFAVVG 337/483
                       .    .    .    .    .    .    .    .    .    .

Sint1          251 SDHEYQVNGKRILGRKTKWGTIEVENTTHCEFAYLRDLLIRTHMQNIKDI 300
                   ||||||||||||||||||||||||||||||||||||||||||||||||||||
KIAA0991/MSF  338/484 SDHEYQVNGKRILGRKTKWGTIEVENTTHCEFAYLRDLLIRTHMQNIKDI 387/533
                       .    .    .    .    .    .    .    .    .    .

Sint1          301 TSNIHFEAYRVKRLNEGNSAMANGI.EKEPEAQEM 334
                   ||.|||||||||||||.|||||: |||||| ||
KIAA0991/MSF  388/534 TSSIHFEAYRVKRLNEGSSAMANGVEEKEPEAPEM 422/568
```

FIG. 7. Comparison of the predicted amino acid sequences encoded by *Sint1* cDNA and a human brain cDNA (KIAA0991; accession no., AB023208) or the human MSF cDNA (accession no., AF123052). The KIAA0991 and MSF sequences are 100% identical in the region shown. Boxed are the GTP-binding motifs. The sequences show 97.0% identity and 97.9% similarity (it should be noted, however, that the KIAA0991 and MSF sequences are 88 and 234 aa residues longer, respectively, than the *Sint1* sequence). Alignment was performed with the Genetics Computer Group program BESTFIT. Vertical lines, identical residues; colons, well-conserved replacements that scored better than 0.5 in the PAM-250 matrix; dots, replacements scoring better than 0.1. The lengths of the *Sint1*, KIAA0991, and MSF sequences are 334, 422, and 568 aa, respectively.

(27), further strengthening the assumption that *Sint1* is a cancer-related gene. The same high degree of homology to a human brain cDNA (KIAA0991)-encoded protein (466 aa) is seen. As mentioned, the integrity of the 5′ end of the *Sint1* cDNA has not been verified, and therefore we cannot exclude the possibility that the full-length *Sint1* cDNA might be several hundred base pairs longer, which again might result in a longer

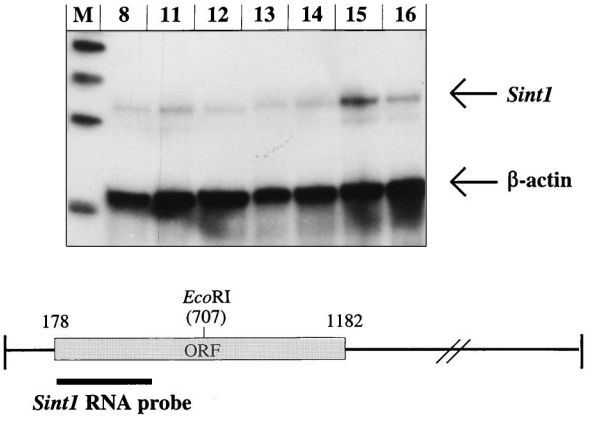

Sint1/β-actin	Tumor 8	Tumor 11	Tumor 12	Tumor 13	Tumor 14	Tumor 15	Tumor 16
Exp. 1	0.05	0.04	0.03	0.04	0.04	0.11	0.04
Exp. 2	0.08	0.05	0.05	0.08	0.09	0.18	0.07

FIG. 8. RNase protection assay. (Top) RNase protection of RNA from seven different SL3-3 MLV-induced tumors assayed with *Sint1* and mouse β-actin RNA probes. Lane M, molecular DNA size markers (200, 300, 400, and 500 bp). Arrows indicate the protected fragments, the sizes of which are 325 bp for *Sint1* and 210 bp for mouse β-actin. (Bottom) Localization of the *Sint1* RNA probe as well as the *Sint1*/β-actin values after quantification of radioactive protected fragments in two experiments (experiment 2 is the one shown at the top).

ORF. In that case, however, the extended region would show a homology of less than 50% to the MSF (or KIAA0991) amino acid sequence. Despite this uncertainty, *Sint1* and MSF seem to represent the same gene in mice and humans, respectively. First, the chromosomal locations match each other. *Sint1* maps to mouse chromosome 11 in an area of human chromosome 17q25 homology (Fig. 3), which corresponds to the location of the MSF gene. Second, results of the Northern blot analyses of *Sint1* and MSF in normal tissues are rather similar (Fig. 4) (27), showing two predominant transcripts of 4.0 and 3.0 kb, the 4.0 kb species being more ubiquitously expressed. In addition, a 1.7-kb transcript is seen in many human tissues, with a relatively high level of expression in heart, liver, skeletal muscle, and kidney (27). Finally, some minor transcripts can be detected in tissues from both organisms. The most prominent difference in expression pattern concerns the expression in skeletal muscle; in mice almost no *Sint1* transcripts are seen; in contrast, in humans skeletal muscle does not seem to be different from other human tissues regarding MSF expression. With respect to the KIAA0991 gene, the nucleotide sequence is 100% identical to the MSF sequence in a long continuous stretch of about 2 kb, suggesting that these two sequences share several exons. Altogether, these observations make us incline to the hypothesis that *Sint1* represents the mouse homolog of MSF and that MSF and KIAA0991 represent splice variants of the human gene. Due to the similarity of expression pattern, it seems reasonable to assume that the *Sint1* cDNA clone characterized here thus represents one of the splice variants in mice.

The genes of the septin family are considered to be involved in cytokinesis and are characterized by a conservation of sequence motifs defining the GTPase superfamily (3, 11). Speculations about the mechanism of leukemogenesis involving members of this family might thus include disturbance of the interactions with the cytoskeletal filaments. GTP binding and hydrolysis may regulate these interactions and/or interactions with other cell cycle proteins.

In summary, we have by a PCR screening of SL3-3-induced tumors identified a common integration site, *Sint1*, and cloned a linked septin-like gene which seems to be affected by the integrated proviruses. The assumption of a role for the *Sint1* gene in leukemogenesis is strongly supported by a recent report of a human homolog (MSF) directly involved in a human acute myeloid leukemia as a fusion partner at a translocation breakpoint (27). However, since only one tumor showed an increased level of *Sint1* RNA, we must leave open the possibility of an effect of the proviral integrations on another still not identified gene(s) at the *Sint1* locus.

ACKNOWLEDGMENTS

We thank Peder Lisby Nørby and Jesper Laursen for helpful technical advice and discussions. Likewise, the technical assistance of Lone Højgaard and Debra J. Gilbert is gratefully acknowledged.

This project was supported by the Danish Cancer Society, the Karen Elise Jensen Foundation, the Danish Natural Sciences and Medical Research Councils, the Danish Biotechnology Programme, DNA Technology A/S, and by the National Cancer Institute, DHHS, under contract with ABL.

REFERENCES

1. **Amtoft, H. W., A. B. Sørensen, C. Bareil, J. Schmidt, A. Luz, and F. S. Pedersen.** 1997. Stability of AML1 (core) site enhancer mutations in T lymphomas induced by attenuated SL3-3 murine leukemia virus mutants. J. Virol. **71:**5080–5087.
2. **Bird, A. P.** 1987. CpG islands as gene markers in the vertebrate nucleus. Trends Genet. **3:**342–347.
3. **Bourne, H. R., D. A. Sanders, and F. McCormick.** 1991. The GTPase superfamily: conserved structure and molecular mechanism. Nature **349:**117–126.
4. **Buchberg, A. M., H. G. Bedigian, N. A. Jenkins, and N. G. Copeland.** 1990. *Evi-2*, a common integration site involved in murine myeloid leukemogenesis. Mol. Cell. Biol. **10:**4658–4666.
5. **Cooper, J. A., and D. P. Kiehart.** 1996. Septins may form a ubiquitous family of cytoskeletal filaments. J. Cell Biol. **134:**1345–1348.
6. **Copeland, N. G., and N. A. Jenkins.** 1991. Development and applications of a molecular genetic linkage map of the mouse genome. Trends Genet. **7:**113–118.
7. **Copeland, N. G., N. A. Jenkins, D. J. Gilbert, J. T. Eppig, L. J. Maltais, J. C. Miller, W. F. Dietrich, A. Weaver, S. E. Lincoln, R. G. Steen, L. D. Stein, J. H. Nadeau, and E. S. Lander.** 1993. A genetic linkage map of the mouse: current applications and future prospects. Science **262:**57–66.
8. **Corcoran, L. M., J. M. Adams, A. R. Dunn, and S. Cory.** 1984. Murine T lymphomas in which the cellular *myc* oncogene has been activated by retroviral insertion. Cell **37:**113–122.
9. **Cuypers, H. T., G. Selten, W. Quint, M. Zijlstra, E. R. Maandag, W. Boelens, P. van Wezenbeek, C. Melief, and A. Berns.** 1984. Murine leukemia virus-induced T-cell lymphomagenesis: integration of proviruses in a distinct chromosomal region. Cell **37:**141–150.
10. **DeMaria, C. T., and G. Brewer.** 1996. AUF1 binding affinity to A+U-rich elements correlates with rapid mRNA degradation. J. Biol. Chem. **271:**12179–12184.
11. **Dever, T. E., M. J. Glynias, and W. C. Merrick.** 1987. GTP-binding domain: three consensus sequence elements with distinct spacing. Proc. Natl. Acad. Sci. USA **84:**1814–1818.
12. **Fletcher, C. F., H. J. Okano, D. J. Gilbert, Y. Yang, C. Yang, N. G. Copeland, N. A. Jenkins, and R. B. Darnell.** 1997. Mouse chromosomal locations of nine genes encoding homologs of human paraneoplastic neurologic disorder antigens. Genomics **45:**313–319.
13. **Graham, M., J. M. Adams, and S. Cory.** 1985. Murine T lymphomas with retroviral inserts in the chromosomal 15 locus for plasmacytoma variant translocations. Nature **314:**740–743.
14. **Hallberg, B., J. Schmidt, A. Luz, F. S. Pedersen, and T. Grundström.** 1991. SL3-3 enhancer factor 1 transcriptional activators are required for tumor formation by SL3-3 murine leukemia virus. J. Virol. **65:**4177–4181.
15. **Hays, E. F., G. Bristol, and S. McDougall.** 1990. Mechanisms of thymic lymphomagenesis by the retrovirus SL3-3. Cancer Res. **50**(Suppl.)**:**5631s–5635s.
16. **Jenkins, N. A., N. G. Copeland, B. A. Taylor, and B. K. Lee.** 1982. Organization, distribution, and stability of endogenous ecotropic murine leukemia virus DNA sequences in chromosomes of *Mus musculus*. J. Virol. **43:**26–36.
17. **Jonkers, J., and A. Berns.** 1996. Retroviral insertional mutagenesis as a strategy to identify cancer genes. Biochim. Biophys. Acta **1287:**29–57.
18. **Justice, M. J., H. C. Morse III, N. A. Jenkins, and N. G. Copeland.** 1994. Identification of *Evi-3*, a novel common site of retroviral integration in mouse AKXD B-cell lymphomas. J. Virol. **68:**1293–1300.
19. **Kumar, S., Y. Tomooka, and M. Noda.** 1992. Identification of a set of genes with developmentally down-regulated expression in the mouse brain. Biochem. Biophys. Res. Commun. **185:**1155–1161.
20. **Larsen, F., G. Gundersen, and H. Prydz.** 1992. Choice of enzymes for mapping based on CpG islands in the human genome. Genet. Anal. Tech. Appl. **9:**80–85.
21. **Liao, X., A. M. Buchberg, N. A. Jenkins, and N. G. Copeland.** 1995. *Evi-5*, a common site of retroviral integration in AKXD T-cell lymphomas, maps near *Gfi-1* on mouse chromosome 5. J. Virol. **69:**7132–7137.
22. **Longtine, M. S., D. J. DeMarini, M. L. Valencik, O. S. Al-Awar, H. Fares, C. De Virgilio, and J. R. Pringle.** 1996. The septins: roles in cytokinesis and other processes. Curr. Opin. Cell Biol. **8:**106–119.
23. **Morishita, K., D. S. Parker, M. L. Mucenski, N. A. Jenkins, N. G. Copeland, and J. N. Ihle.** 1988. Retroviral activation of a novel gene encoding a zinc finger protein in IL-3-dependent myeloid leukemia cell lines. Cell **54:**831–840.
24. **Morrison, H. L., B. Soni, and J. Lenz.** 1995. Long terminal repeat enhancer core sequences in proviruses adjacent to c-*myc* in T-cell lymphomas induced by a murine retrovirus. J. Virol. **69:**446–455.
25. **Nakatsuru, S., K. Sudo, and Y. Nakamura.** 1994. Molecular cloning of a novel human cDNA homologous to CDC10 in *Saccharomyces cerevisiae*. Biochem. Biophys. Res. Commun. **202:**82–87.
26. **Neufeld, T. P., and G. M. Rubin.** 1994. The *Drosophila peanut* gene is required for cytokinesis and encodes a protein similar to yeast putative bud neck filament proteins. Cell **77:**371–379.
27. **Osaka, M., J. D. Rowley, and N. J. Zeleznik-Le.** 1999. MSF (MLL septin-like fusion), a fusion partner gene of MLL, in a therapy-related acute myeloid leukemia with a t(11;17)(q23;q25). Proc. Natl. Acad. Sci. USA **96:**6428–6433.
28. **Rajan, L., and J. P. Dudley.** 1997. An MMTV integration site maps near the distal end of mouse chromosome 11. Mamm. Genome **8:**295–296.
29. **Rosenberg, N., and P. Jolicoeur.** 1997. Retroviral pathogenesis, 475–586. *In* J. M. Coffin, S. H. Hughes, and H. E. Varmus (ed.), Retroviruses. Cold Spring Harbor Laboratory Press, Cold Spring Harbor, N.Y.
30. **Sambrook, J., E. F. Fritsch, and T. Maniatis.** 1989. Molecular cloning: a laboratory manual, 2nd ed. Cold Spring Harbor Laboratory, Cold Spring Harbor, N.Y.
31. **Selten, G., H. T. Cuypers, and A. Berns.** 1985. Proviral activation of the

putative oncogene *Pim*-1 in MuLV induced T-cell lymphomas. EMBO J. **4:**1793–1798.
32. **Shaw, G., and R. Kamen.** 1986. A conserved AU sequence from the 3′ untranslated region of GM-CSF mRNA mediates selective mRNA degradation. Cell **46:**659–667.
33. **Shen-Ong, G. L. C., H. C. Morse III, M. Potter, and F. Muchinsky.** 1986. Two modes of c-*myb* activation in virus-induced mouse myeloid tumors. Mol. Cell. Biol. **6:**380–392.
34. **Sørensen, A. B., M. Duch, P. Jørgensen, and F. S. Pedersen.** 1993. Amplification and sequence analysis of DNA flanking integrated proviruses by a simple two-step polymerase chain reaction method. J. Virol. **67:**7118–7124.
35. **Sørensen, A. B., M. Duch, H. W. Amtoft, P. Jørgensen, and F. S. Pedersen.** 1996. Sequence tags of provirus integration sites in DNAs of tumors induced by the murine retrovirus SL3-3. J. Virol. **70:**4063–4070.
36. **Steffen, D.** 1984. Proviruses are adjacent to c-*myc* in some murine leukemia virus-induced lymphomas. Proc. Natl. Acad. Sci. USA **81:**2097–2101.
37. **Tsichlis, P. N., B. M. Shephard, and S. E. Bear.** 1989. Activation of the *Mlvi*-1/*mis*1/*pvt*-1 locus in Moloney murine leukemia virus-induced T-cell lymphomas. Proc. Natl. Acad. Sci. USA **86:**5487–5491.
38. **van Lohuizen, M., and A. Berns.** 1990. Tumorigenesis by slow-transforming retroviruses—an update. Biochim. Biophys. Acta **1032:**213–235.
39. **Wolff, L.** 1996. Myb-induced transformation. Crit. Rev. Oncog. **7:**245–260.